TEMPERATURE IMAGING USING ULTRASONIC CHANGE IN BACKSCATTERED ENERGY

Jie Li

Abstract

Conducting turkey specimens in non-uniform heating experiments with Terason 3000 system and TI (temperature imaging) system. Total heating time was 1200 sec, with a 30 sec interval between image acquisitions, tissue temperature was monitored with thermocouples. We take frame 1, frame 10, frame 20 and frame 40 for instance, and their corresponding experiment times are 30 seconds, 300 seconds, 600 seconds and 1200 seconds respectively.

Uniform probability distribution function(pdf) change in backscattered energy(CBE) images contain a plenty of noises, so we generate Ratio pdf CBE images to eliminate noises and get smooth images. In order to decrease processing time, we introduce CBE block images over 2*2/ 4*4/ 6*6 mm on baseline results and corresponding CBE variation curves for each block. Then using interpolation to generate smoother CBE images over 2*2/ 4*4/ 6*6 mm.

I. INTRODUCTION

According to clinical finding, thermal therapy is a new way to kill cancer cells or destroy a tumor, and it plays an important role in improving treatment. In order to induce a desire biological response, the aim of thermal therapy is to change tissue temperature in a targeted region over time. On the purpose to increase the efficacy, it is necessary for us to require feedback of therapies. Therefore, a number of therapies use imaging to monitor the treatment [1]. Both Magnetic resonance (MR) and ultrasound (US) imaging are possible methods to measure tissue temperature and generate images. MRI is known for its advantages like multi-parameter imaging, zero-radioactivity and high resolution over other methods,and it has already been used in some commercial MR-guided high intensity focused ultrasound systems.

However, its exorbitant price makes people flinched, and it takes up a lot of space for devices, the survey found [2]. In contrast, ultrasound is comparatively low-cost, non-ionizing, compact and flexible [3]. The non-invasive thermometer, ultrasound, has the following three usages, 1) echo-shifts based thermal strain, 2) acoustic attenuation coefficient, and 3) change in backscattered energy (CBE) [2], [4]. For these reasons, it widespread use in medical research and clinical applications in recent years [4], [2]. Echo strain is directly proportional to the local change in the speed of sound caused by temperature change.So in the last decade, researchers tried to use speed of sound (SOS) maps to infer temperature distributions. Since the measurement process is too complicated and tissue type has a great effect on the temperature, this method has not been applied to clinic, although this method has been successful in calibrated, homogeneous tissue phantoms. In soft tissues, two research groups have found that attenuation was highly dependent on temperature above 50°C and attenuation caused by tissue damage [5], [6]. But it is not suitable for moderate-temperature hyperthermia due to the high temperature [7].

We generate temperature images with non-uniform heat source and thermocouples. In laboratory, the non-uniform heat source is a central hot-water source, which is a tube with hot water crossing the center of a turkey specimen. Because we use turkey specimens which are static specimens in this experiment, we do not need to consider motion compensation for $vivo$ studies [8], [9]. Thus, the change in backscattered energy is based on changes in speed of sound and density of the medium compared to their values in sub-wavelength inhomogeneties (scatterers) within the medium. The CBE at any temperature T with respect to its value at some reference temperature T_R is

$$CBE(T) = \frac{\alpha(T_R)\eta(T)[1 - e^{-2\alpha(T)x}]}{\alpha(T)\eta(T_R)[1 - e^{-2\alpha(T_R)x}]} \quad ,$$

where, $\alpha(T)$ is the attenuation within the tissue volume and $\eta(T)$ is the backscatter coefficient of the tissue volume. Ignoring the effects of small changes in wave number ($< 1.5\%$) with temperature, [10].

$$\frac{\eta(T)}{\eta(T_R)} = \frac{(\frac{(\rho_m c(T)_m^2 - \rho_s c(T)_s^2}{\rho_s c(T)_s^2})^2 + \frac{1}{3}(\frac{(3\rho_s - 3\rho_m)}{2\rho_s + \rho_m})^2}{(\frac{(\rho_m c(T_R)_m^2 - \rho_s c(T_R)_s^2}{\rho_s c(T_R)_s^2})^2 + \frac{1}{3}(\frac{(3\rho_s - 3\rho_m)}{2\rho_s + \rho_m})^2} \quad ,$$

where ρ and c are the density and speed of sound of the scatterer s and medium m. In CBE-based temperature estimation method, CBE can be used to reflect temperature change. Furthermore, in 1D studies, the CBE can be divided into positive CBE and negative CBE. And the standard deviation of positive and negative CBE is the CBE value we want [4].

$$PCBE = \frac{\int_1^\infty z f_Z(z)dz}{\int_1^\infty f_Z(z)dz}; \quad NCBE = \frac{\int_0^1 z f_Z(z)dz}{\int_0^1 f_Z(z)dz} \quad .$$

Non-invasive CBE temperature imaging can be done during non-uniform heating in real time [11]. At present, CBE at each pixel in a non-uniformly heated region is formed as that region is moved horizontally and vertically over an image. This process is slow. One objective of this study was to determine whether or not finding one CBE value over the region, then interpolating these block CBE values to form the CBE image was comparable to the result obtained by moved region one pixel at a time. In addition, assuming all CBE values are equally likely, uniform probability density function (updf) introduces noise from outlier values of CBE. We have shown previously that our stochastic-signal processing framework could reduce effects of noise on CBE in simulation using a ratio probability density function (rpdf) [12]. A second objective of this study was to characterize the potential noise reduction using the rpdf experimentally.

II. Methods

Use td714_nonrigid4.mat with height equals 6 and width equals 6 to generate the baseline results: uniform and ratio pdf at each pixel. We take frame 1, frame 10, frame 20 and frame 40 for instance, and their corresponding experiment times are 30 seconds, 300 seconds, 600 seconds and 1200 seconds respectively. Use height equals 2 and width equals 2, height equals 4 and width equals 4, and height equals 6 and width equals 6 to generate blocks and save results as td714_block2, td714_block4, td714_block6 respectively. The CBE value of every block is the average value of pixel CBE values in this block area. Then do interpolation by interp2 function, which returns the interpolated values on a refined grid formed by dividing the interval between sample values once in each dimension. In this way, we can generate interpolate uniform CBE images and interpolate rpdf CBE images. These images look like pixel uniform CBE images and pixel rpdf CBE images, but with less noises. Plot CBE variation curves for every block. Analyse these lines, find the first and second order polynomials to best fit data. Test fitting accuracy.

When we generate blocks, in order to make sure that every block contains the same number of CBE values, we give up some values on the top and on the left and right sides. For instance, when we choose height equals 6 and width equals 6, we abandon 125 rows on the top and 1 column on both left and right sides (the total is 2 columns), then generate 5*4 (20) blocks, and every block contains 3740 CBE values. When we choose height equals 4 and width equals 4, we abandon 123 rows on the top, 6 columns on left and 5 columns on right sides (the total is 11 columns), then generate 7*6 (42) blocks, and every block contains 1625 CBE values. When we choose height equals 2 and width equals 2. We abandon 5 rows on the top and 2 columns on both left and right sides (the total is 4 columns), then generate 14*14 (196) blocks, and every block contains 434 CBE values.

III. Results

A. Baseline Results: Uniform and Ratio pdf with ht&wd=6 mm ROI at each Pixel

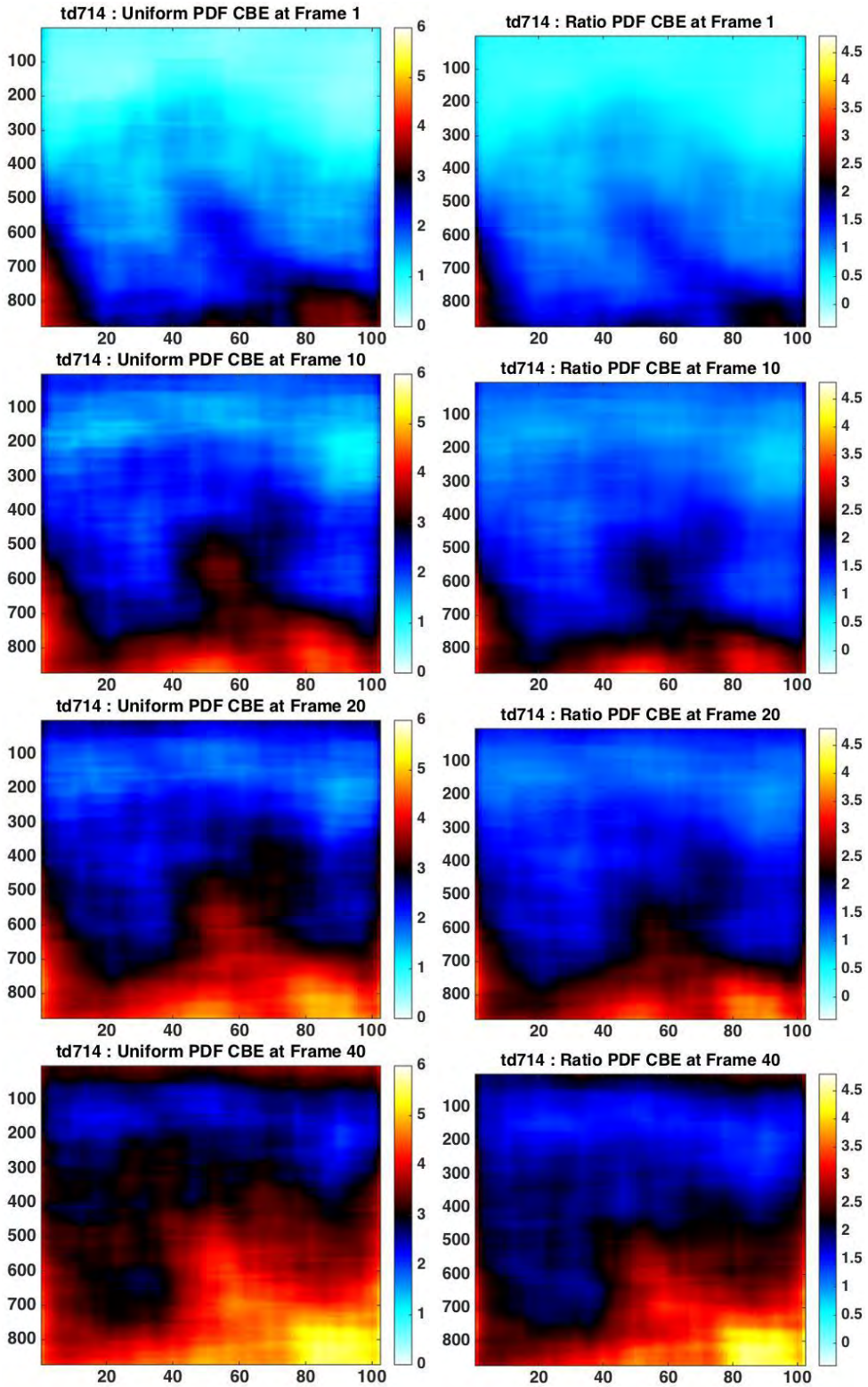

Fig. 1. Left) Uniform pdf cbe. Right) Ratio pdf cbe. Cbe over 6 x 6 mm regions and shown at frames # 1 10 20 40. Color scale is in dB.

B. PDF & Block & Interpolation over 6 x 6 mm

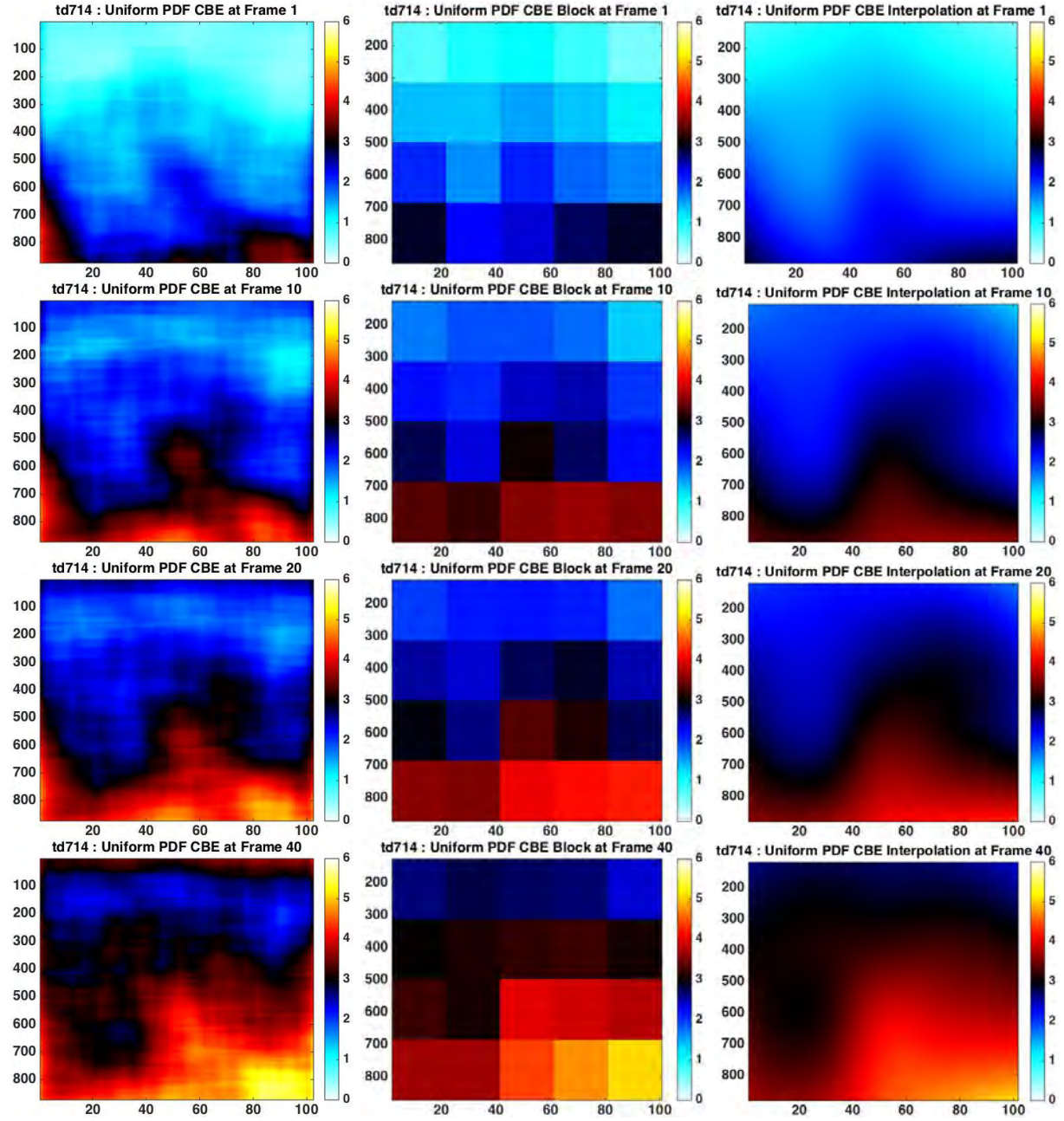

Fig. 2. Left) Uniform pdf cbe. Middle) Uniform pdf cbe block. Right) Uniform pdf cbe interpolation. Uniform pdf cbe over 6 x 6 mm regions, uniform pdf cbe block over 6 x 6 mm and shown at frames # 1 10 20 40. Color scale is in dB.

1) Uniform pdf over 6 x 6 mm ROIs at each Pixel & over 6 x 6 mm Blocks & Interpolation:

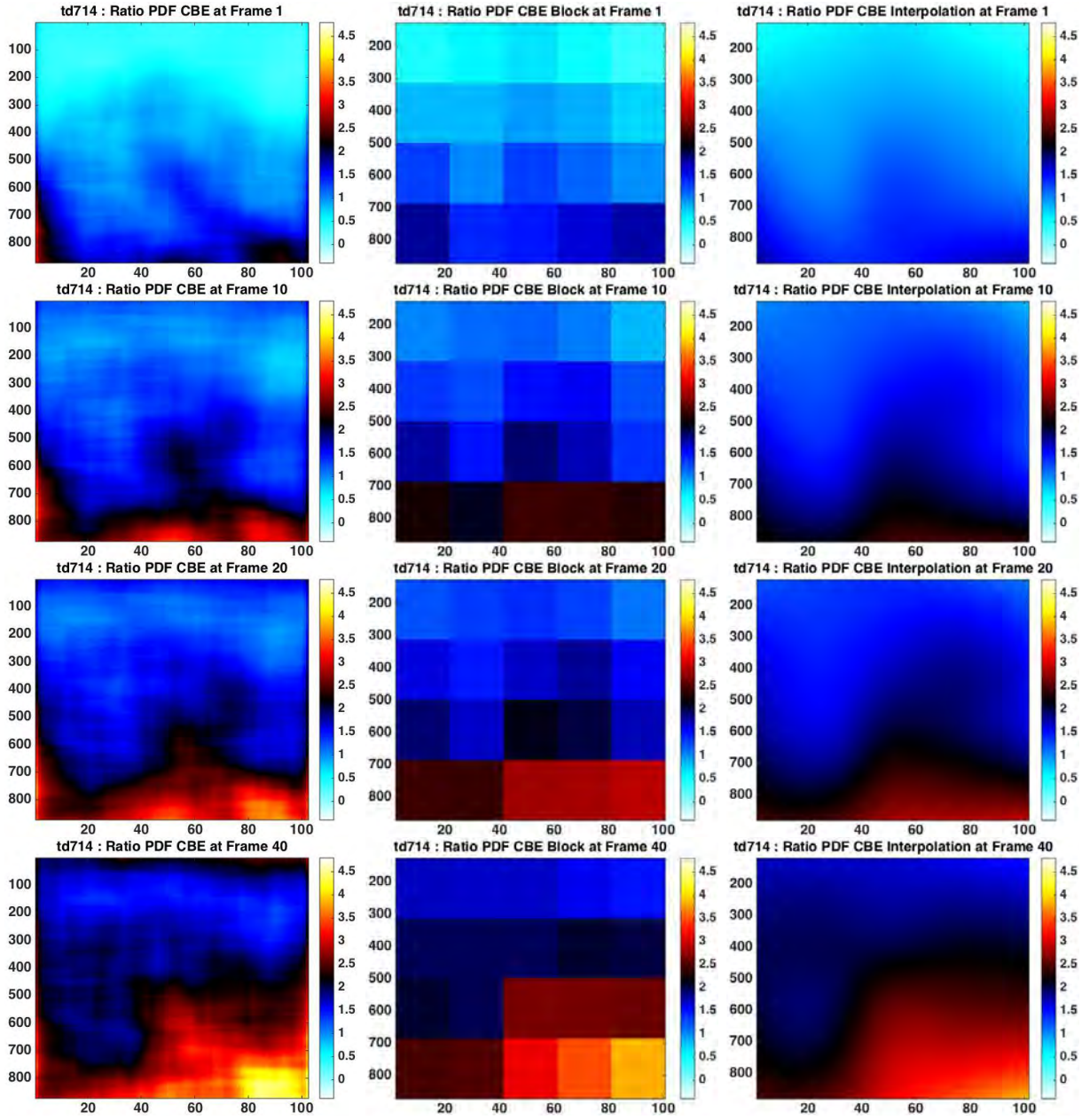

Fig. 3. Left) Ratio pdf cbe. Middle) Ratio pdf cbe block. Right) Ratio pdf cbe interpolation. Ratio pdf cbe over 6 x 6 mm regions, ratio pdf cbe block over 6 x 6 mm and shown at frames # 1 10 20 40. Color scale is in dB.

2) Ratio pdf over 6 x 6 mm ROIs at each Pixel & over 6 x 6 mm Blocks & Interpolation:

3) Uniform and Ratio PDF Block CBE Variation over 6 x 6 mm: Generate every block's CBE from experiment time 0 sec to 1200 sec (frame 1 to frame 40).

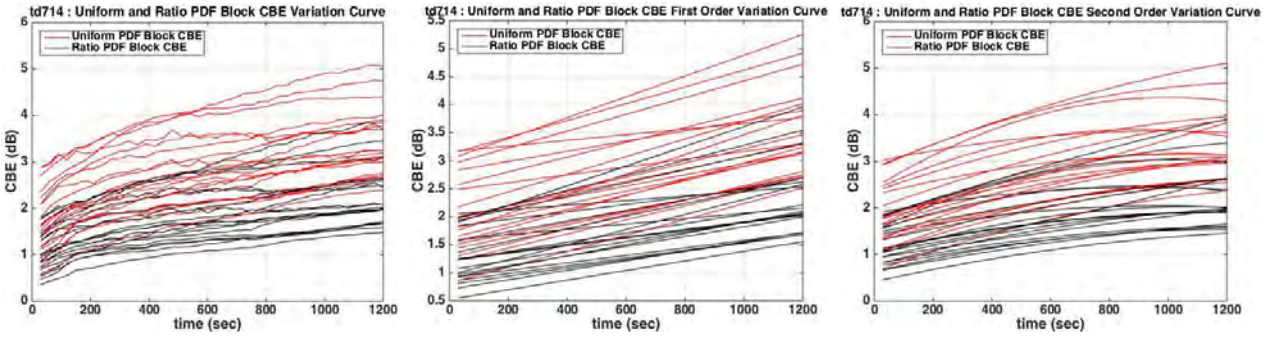

Fig. 4. Left) Block CBE variation curves over 6 x 6 mm regions. Middle)Block CBE variation curves first order polynomial fitting over 6 x 6 mm regions. Right) Block CBE variation curves second order polynomial fitting over 6 x 6 mm regions.

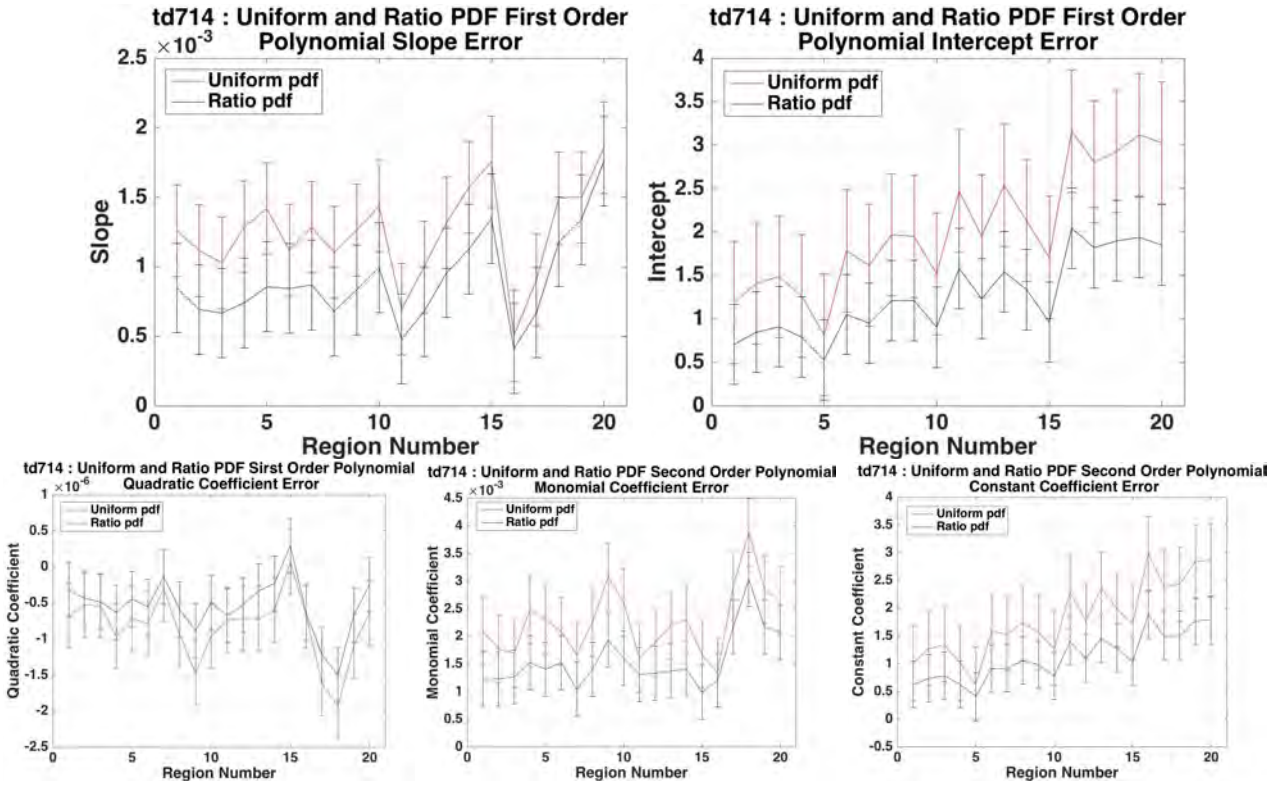

Fig. 5. Top) Uniform and ratio pdf block CBE variation curves first order polynomial fitting coefficients error over 6 x 6 mm regions. Bottom) Uniform and ratio pdf block CBE variation curves second order polynomial fitting coefficients error over 6 x 6 mm regions.

4) Uniform and Ratio PDF Block CBE Variation Curves First and Second Order Polynomial Fitting Coefficients Error over 6 x 6 mm:

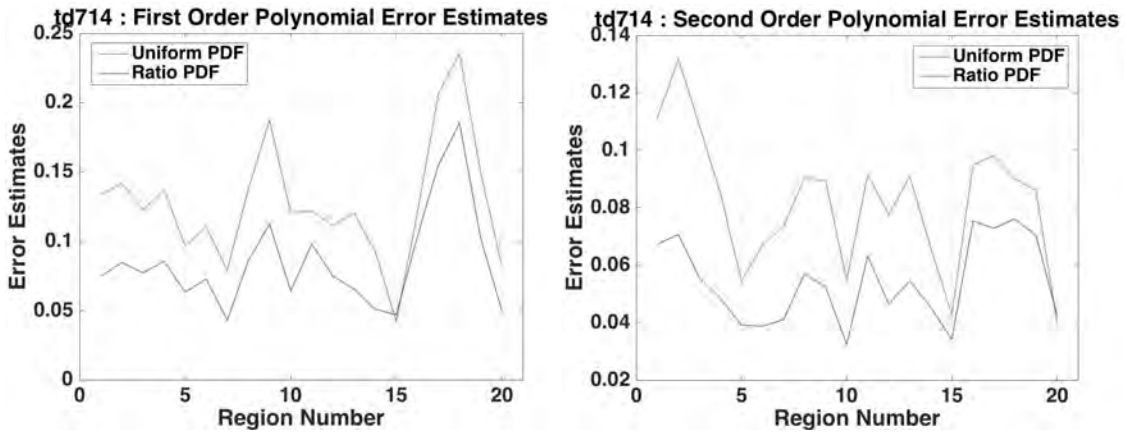

Fig. 6. Left) Uniform pdf and ratio pdf block CBE variation curves first order polynomial error estimates over 6 x 6 mm regions. Right) Uniform pdf and ratio pdf block CBE variation curves second order polynomial error estimates over 6 x 6 mm regions.

5) Uniform and Ratio PDF Block CBE Variation Curves First and Second Order Polynomial Fitting Error Estimates over 6 x 6 mm:

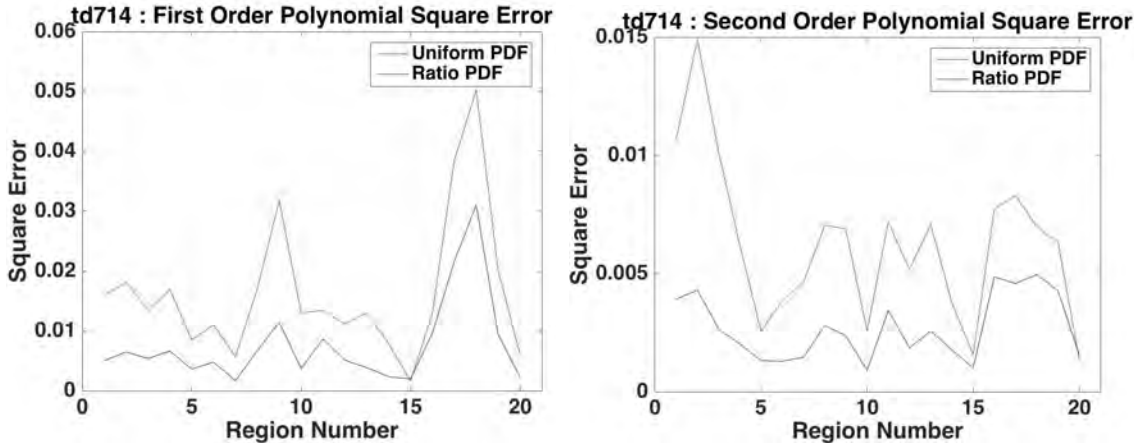

Fig. 7. Left) Uniform pdf and ratio pdf block CBE variation curves first order polynomial fitting square error over 6 x 6 mm regions. Right) Uniform pdf and ratio pdf block CBE variation curves second order polynomial fitting square error over 6 x 6 mm regions.

6) Uniform and Ratio PDF Block CBE Variation Curves First and Second Order Polynomial Fitting Error Square over 6 x 6 mm:

C. PDF & Block & Interpolation over 4 x 4 mm

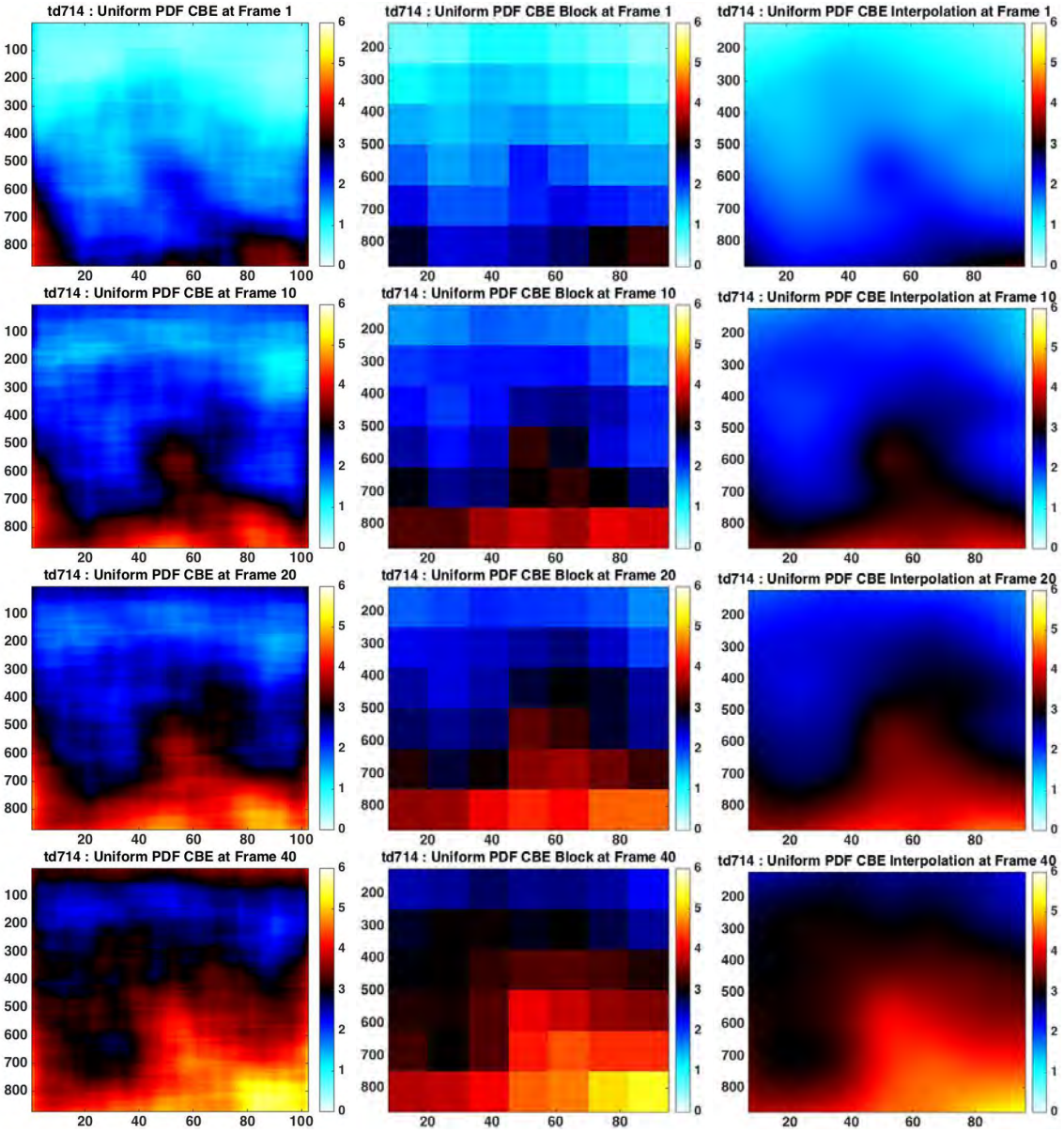

Fig. 8. Left) Uniform pdf cbe. Middle) Uniform pdf cbe block. Right) Uniform pdf cbe interpolation. Uniform pdf cbe over 6 x 6 mm regions, uniform pdf cbe block over 4 x 4 mm and shown at frames # 1 10 20 40. Color scale is in dB.

1) Uniform pdf over 6 x 6 mm ROIs at each Pixel & over 4 x 4 mm Blocks & Interpolation:

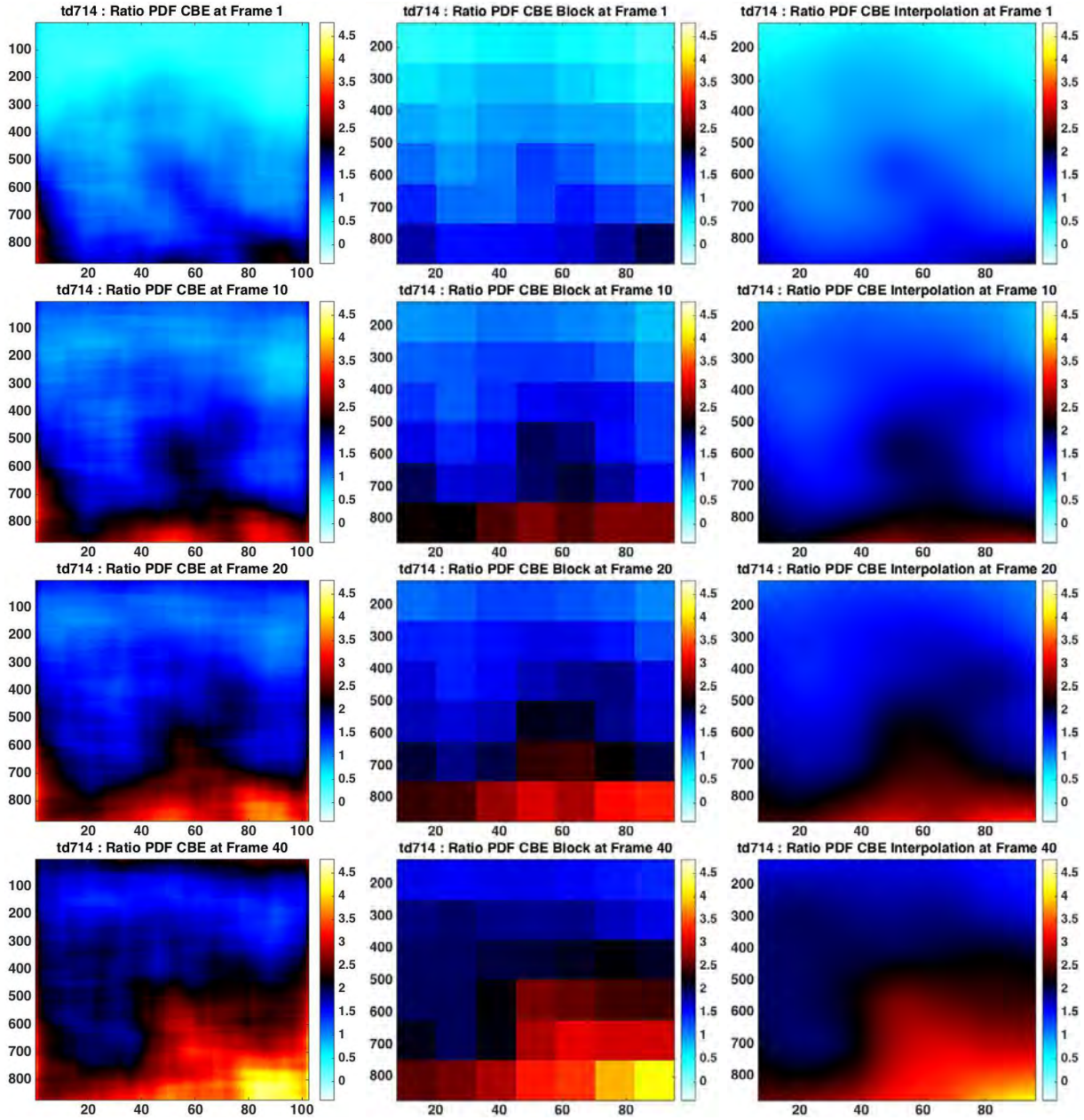

Fig. 9. Left) Ratio pdf cbe. Middle) Ratio pdf cbe block. Right) Ratio pdf cbe interpolation. Ratio pdf cbe over 6 x 6 mm regions, ratio pdf cbe block over 4 x 4 mm and shown at frames # 1 10 20 40. Color scale is in dB.

2) Ratio pdf over 6 x 6 mm ROIs at each Pixel & over 4 x 4 mm Blocks & Interpolation:

3) Uniform and Ratio PDF Block CBE Variation over 4 x 4 mm: Generate every block's CBE from experiment time 0 sec to 1200 sec (frame 1 to frame 40).

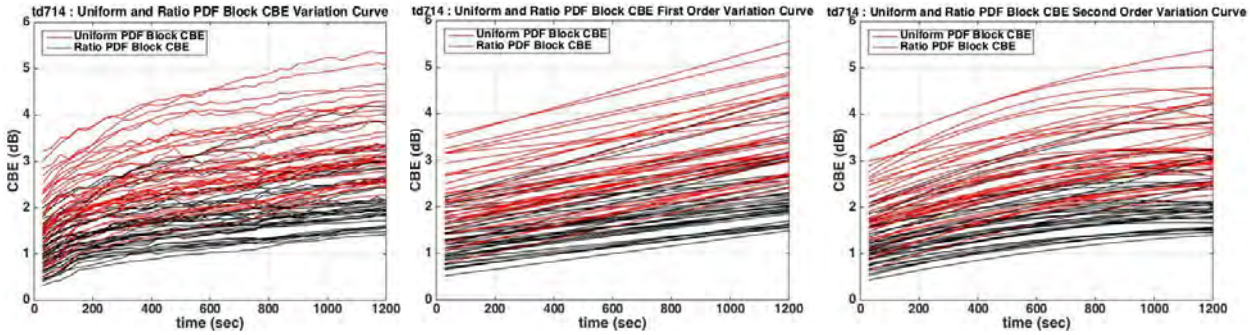

Fig. 10. Left) Block CBE variation curves over 4 x 4 mm regions. Middle)Block CBE variation curves first order polynomial fitting over 4 x 4 mm regions. Right) Block CBE variation curves second order polynomial fitting over 4 x 4 mm regions.

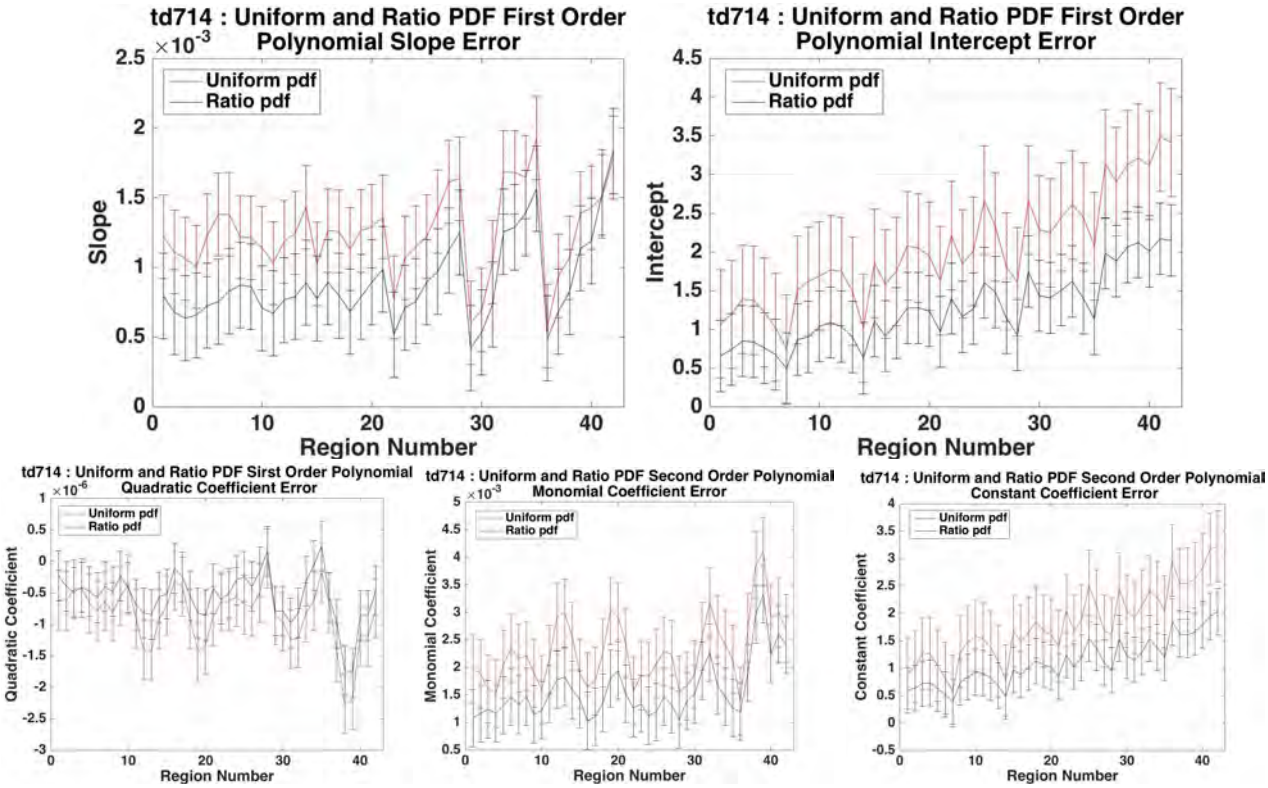

Fig. 11. Top) Uniform and ratio pdf block CBE variation curves first order polynomial fitting coefficients error over 4 x 4 mm regions. Bottom) Uniform and ratio pdf block CBE variation curves second order polynomial fitting coefficients error over 4 x 4 mm regions.

4) Uniform and Ratio PDF Block CBE Variation Curves First and Second Order Polynomial Fitting Coefficients Error over 4 x 4 mm:

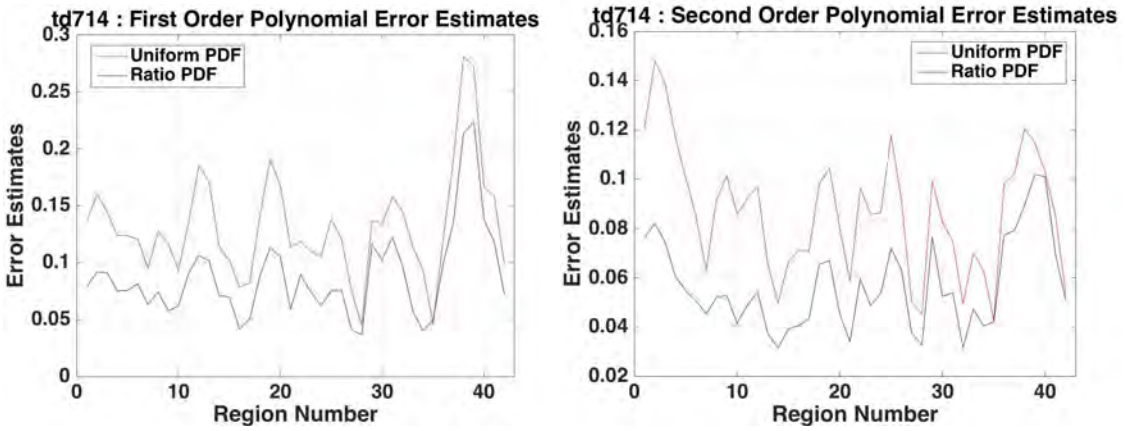

Fig. 12. Left) Uniform pdf and ratio pdf block CBE variation curves first order polynomial error estimates over 4 x 4 mm regions. Right) Uniform pdf and ratio pdf block CBE variation curves second order polynomial error estimates over 4 x 4 mm regions.

5) Uniform and Ratio PDF Block CBE Variation Curves First and Second Order Polynomial Fitting Error Estimates over 4 x 4 mm:

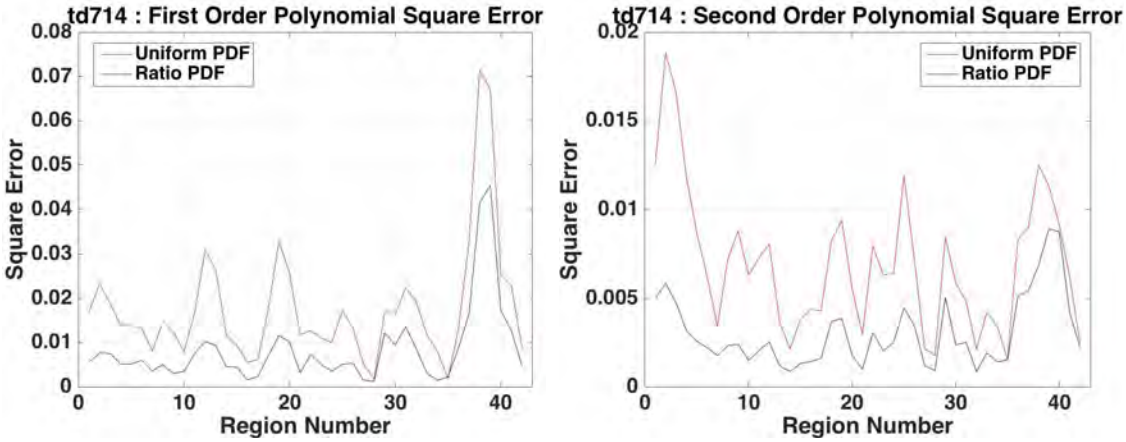

Fig. 13. Left) Uniform pdf and ratio pdf block CBE variation curves first order polynomial fitting square error over 4 x 4 mm regions. Right) Uniform pdf and ratio pdf block CBE variation curves second order polynomial fitting square error over 4 x 4 mm regions.

6) Uniform and Ratio PDF Block CBE Variation Curves First and Second Order Polynomial Fitting Error Square over 4 x 4 mm:

D. PDF & Block & Interpolation over 2 x 2 mm

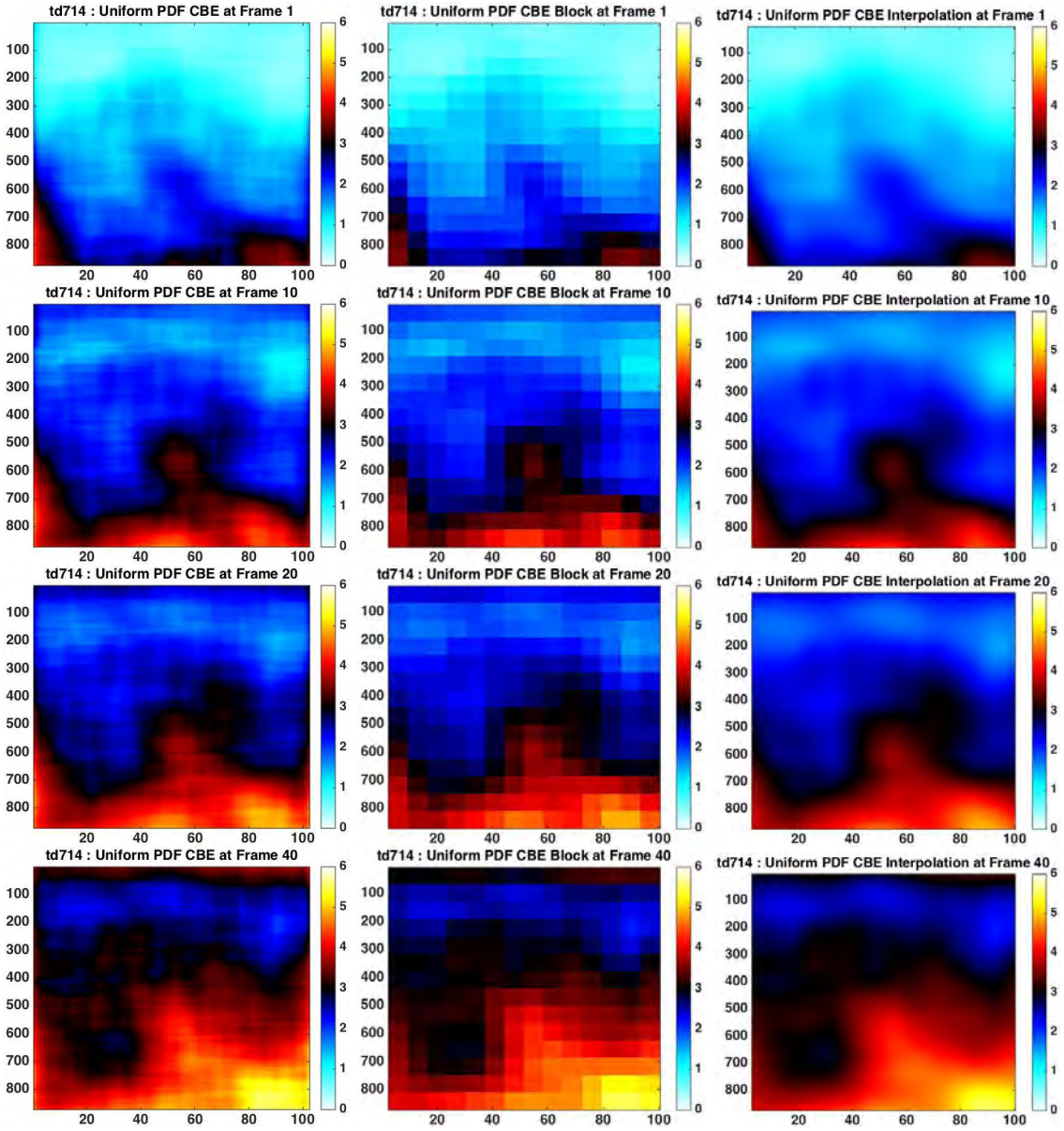

Fig. 14. Left) Uniform pdf cbe. Middle) Uniform pdf cbe block. Right) Uniform pdf cbe interpolation. Uniform pdf cbe over 6 x 6 mm regions, uniform pdf cbe block over 2 x 2 mm and shown at frames # 1 10 20 40. Color scale is in dB.

1) Uniform pdf over 6 x 6 mm ROIs at each Pixel & over 2 x 2 mm Blocks & Interpolation:

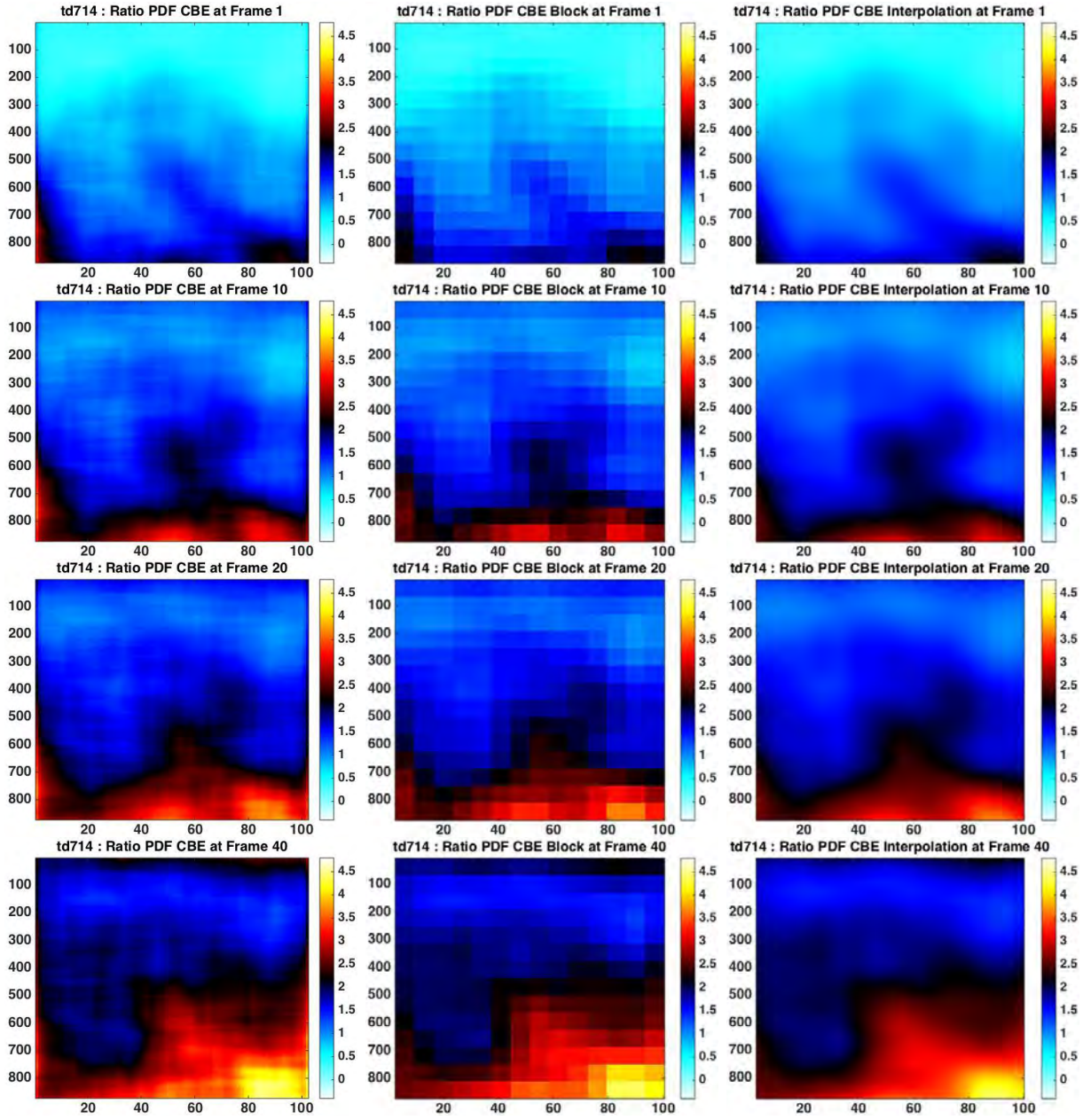

Fig. 15. Left) Ratio pdf cbe. Middle) Ratio pdf cbe block. Right) Ratio pdf cbe interpolation. Ratio pdf cbe over 6 x 6 mm regions, ratio pdf cbe block over 2 x 2 mm and shown at frames # 1 10 20 40. Color scale is in dB.

2) Ratio pdf over 6 x 6 mm ROIs at each Pixel & over 2 x 2 mm Blocks & Interpolation:

3) Uniform and Ratio PDF Block CBE Variation Curves over 2 x 2 mm: Generate every block's CBE from experiment time 0 sec to 1200 sec (frame 1 to frame 40).

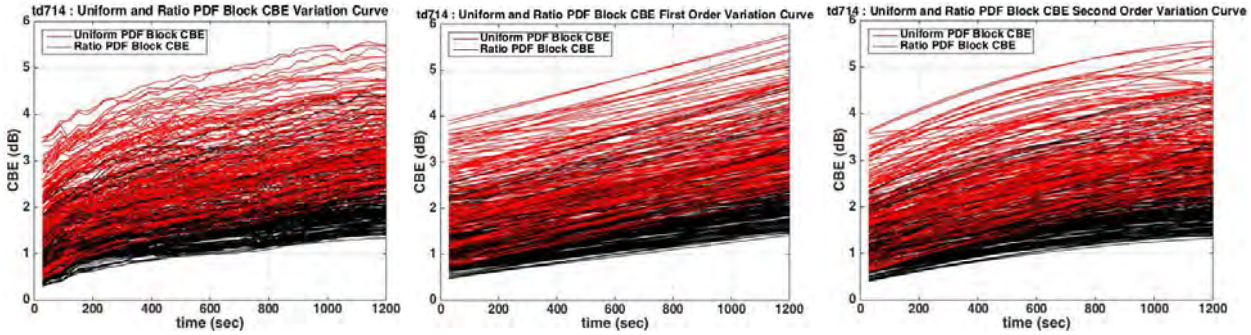

Fig. 16. Left) Block CBE varition curves over 2 x 2 mm regions. Middle)Block CBE variation curves first order polynomial fitting over 2 x 2 mm regions. Right) Block CBE variaxtion curves second order polynomial fitting over 2 x 2 mm regions.

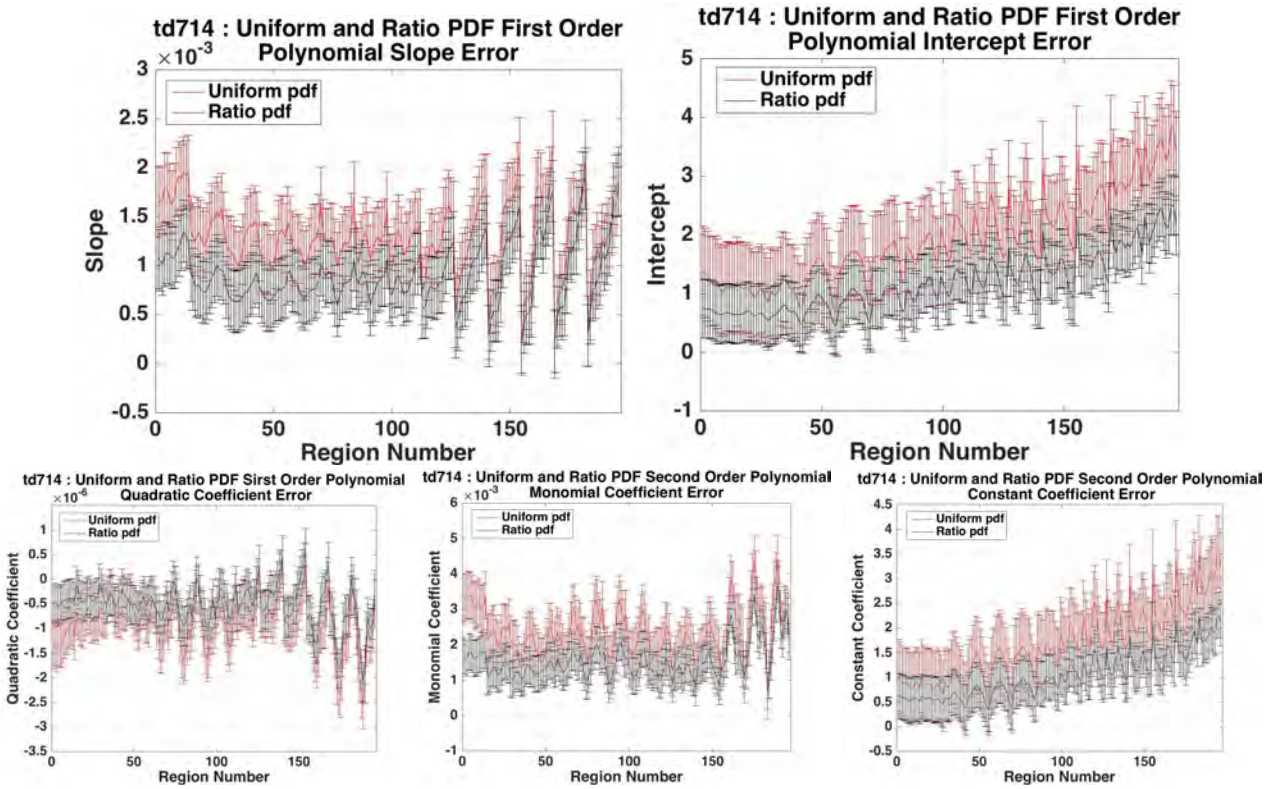

Fig. 17. Top) Uniform and ratio pdf block CBE variation curves first order polynomial fitting coefficients error over 2 x 2 mm regions. Bottom) Uniform and ratio pdf block CBE variation curves second order polynomial fitting coefficients error over 2 x 2 mm regions.

4) Uniform and Ratio PDF Block CBE Variation Curves First and Second Order Polynomial Fitting Coefficients Error over 2 x 2 mm:

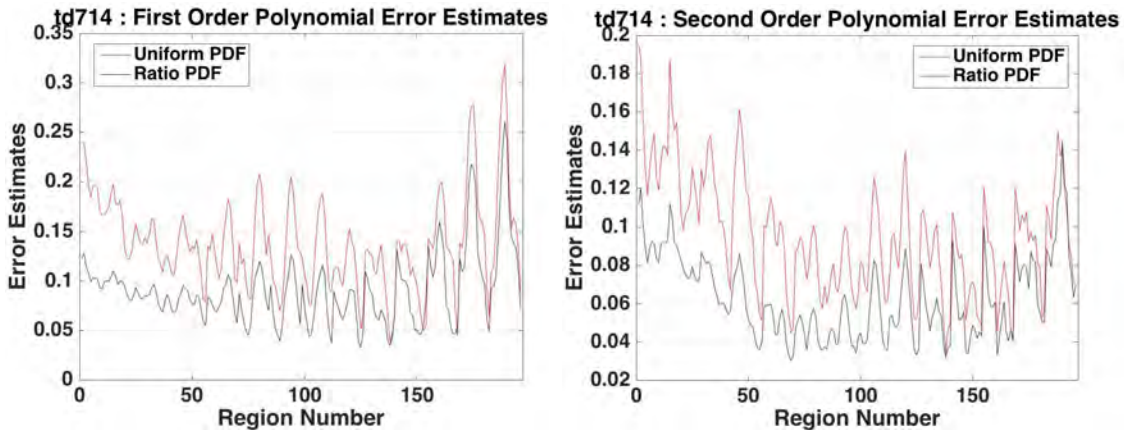

Fig. 18. Left) Uniform pdf and ratio pdf block CBE variation curves first order polynomial error estimates over 2 x 2 mm regions. Right) Uniform pdf and ratio pdf block CBE variation curves second order polynomial error estimates over 2 x 2 mm regions.

5) Uniform and Ratio PDF Block CBE Variation Curves First and Second Order Polynomial Fitting Error Estimates over 2 x 2 mm:

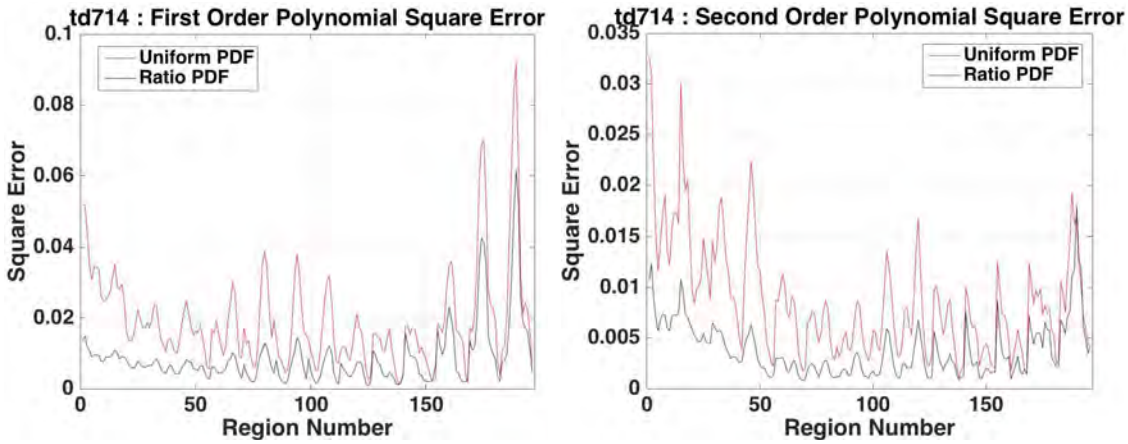

Fig. 19. Left) Uniform pdf and ratio pdf block CBE variation curves first order polynomial fitting square error over 2 x 2 mm regions. Right) Uniform pdf and ratio pdf block CBE variation curves second order polynomial fitting square error over 2 x 2 mm regions.

6) Uniform and Ratio PDF Block CBE Variation Curves First and Second Order Polynomial Fitting Error Square over 2 x 2 mm:

IV. Discussion

Ultrasound is currently the most common way of treating cancer. CBE is a good method to show the temperature distribution and change on a tissue. Both pixel and block CBE images can represent the tissue temperature. While because of the size of pixel and block, processing times in these two methods have significant difference. Pixel CBE images contain more details, it displays pixels one by one, but with a plenty of noises. Block CBE images block temperature, and it shows the basic temperature distribution. Similarly, both uniform and ratio pdf CBE images can represent the tissue temperature. However, because of the logarithmic operation ratio pdf CBE images' distribution is more concentrated, and that's why it contains less noises.

When we generate uniform pdf CBE block and ratio pdf CBE block, in order to make sure every block contains the same number of CBE values, we abandon some rows on the top and some columns on both left and right sides. This will make it a little bit different. However, top rows are far from the heating source, ignoring some cold part with low CBE values will not affect the overall figure. In the meanwhile, we pay close attention to the distribution of CBE values, so both left and right sides will not destroy the integrity of figures. That's how we choose the number of CBE values in every block.

As to first and second order polynomial fitting. Since we use non-uniform heat source, the temperature change is not linear. The far the tissue is, the slower it gets heat. As we all know, tissue consists of muscle, fat, meridians and others, and these elements have different conductivities, so they can not be uniformly heated. Meanwhile, as the temperature rises, a same area tissue needs more heat to increase 1 degree. In summary, second order polynomial can describe the temperature change better.

V. Conclusions

For two problems we raised in the introduction, we can make conclusions now. We do find a way to calculate the CBE value over the region, then interpolations. In this method, we use the mean of CBE values in one block area to represent this block's CBE value, so we reproduce the CBE images by moving regions block by block, which can also decrease processing time. CBE block images reproduce images in a modular form. Interpolation CBE images are similar to their pixel CBE images, but more smooth and transitivity. In analyze, we use uniform pdf CBE block and its interpolation to reproduce uniform pdf CBE image. From 6*6 mm to 4*4 mm, then to 2*2 mm blocks, we can see the smaller the size we choose, the more blocks will be generated in CBE block images, which means more details will be kept and new images are closer to the original. Over 6*6 mm, the total generating time is 3.532799 seconds. We have 5*4 (20) blocks. Even though block images remain the main information, we still lose some details. What's more, interpolation images are not very accurate. We can say the difference by the naked eye. Over 4*4 mm, the total generating time is 3.638547 seconds. We have 7*6 (42) blocks. In this case, CBE block images can describe CBE pixel images preliminarily. Interpolate images have a clear boundary and obvious gradient. Over 2*2 mm, the total generating time is 3.955436 seconds. We have 14*14 (196) blocks. In this situation, we have enough blocks to save details of pixel CBE images, so interpolate CBE images look very similar to pixel CBE images. As a conclusion, we can believe interpolate CBE images reproduce pixel CBE images, and with less noises.

As to the second objective of this study, we generate ratio pdf CBE images by using logarithm whose base is 10. Because logarithm is the inverse operation to exponentiation, so it reduces numerical range. A more compact numerical distribution leads to smooth transition among data,reducing the potential noise. From the baseline results, we can find ratio pdf CBE images are smoother, and contain less noises than uniform pdf CBE images. Combined with objective one, we use ratio pdf CBE block and its interpolation to reproduce ratio pdf CBE image.

Besides, we can learn from CBE variance curves that uniform pdf block CBE range is wider than ratio pdf block CBE. Over 6*6 mm, the range of uniform pdf block CBE is about 1.75dB (3.4181-1.6667), while for ratio pdf block CBE, it's about 1.24dB (2.2696-1.0304). Over 4*4 mm, the range of uniform pdf block CBE is about 1.76dB (3.4056-1.6441), while for ratio pdf block CBE, it's about 1.24dB (2.2571-1.0163). Over 2*2 mm, the range of uniform pdf block CBE is about 1.82dB (3.3325-1.5134), while for ratio pdf block CBE, it's about 1.26dB (2.2003-0.9360).

Furthermore, we finish first and second order polynomial fitting. For uniform pdf block CBE variation curves fitting over 6*6 mm region,in first order polynomial, the mean of slope is 0.0012, and the mean of intercept is 2.0425; the standard standard deviation of slope is 3.2988e-04, and the standard deviation of intercept is 0.7028. In second order polynomial, the mean of quadratic coefficient is -8.3045e-07, the mean of monomial coefficient is 0.0023, and the mean of constant coefficient is 1.8280; the standard deviation of quadratic coefficient is 4.4809e-07, the standard deviation of monomial coefficient is 6.1205e-04, and the standard deviation of constant coefficient is 0.6663. For ratio pdf block CBE variation curves fitting,in first order polynomial, the mean of slope is 8.9843e-04, and the mean of intercept is 1.2661; the standard standard deviation of slope is 3.2242e-04, and the standard deviation of intercept is 0.4615. In second order polynomial, the mean of quadratic coefficient is -5.3782e-07, the mean of monomial coefficient is 0.0016, and the mean of constant coefficient is 1.1272; the standard deviation of quadratic coefficient is 3.7878e-07, the standard deviation of monomial coefficient is 4.8964e-04, and the standard deviation of constant coefficient is 0.4251.

For uniform pdf block CBE variation curves fitting over 4*4 mm region,in first order polynomial, the mean of slope is 0.0012, and the mean of intercept is 2.0332; the standard standard deviation of slope is 2.9825e-04, and the standard deviation of intercept is 0.6997. In second order polynomial, the mean of quadratic coefficient is -8.5319e-07, the mean of monomial

coefficient is 0.0023, and the mean of constant coefficient is 1.8128; the standard deviation of quadratic coefficient is 4.6814e-07, the standard deviation of monomial coefficient is 6.1820e-04, and the standard deviation of constant coefficient is 0.6527. For ratio pdf block CBE variation curves fitting,in first order polynomial, the mean of slope is 8.9399e-04, and the mean of intercept is 1.2599; the standard standard deviation of slope is 3.0566e-04, and the standard deviation of intercept is 0.4599. In second order polynomial, the mean of quadratic coefficient is -5.5650e-07, the mean of monomial coefficient is 0.0016, and the mean of constant coefficient is 1.1162; the standard deviation of quadratic coefficient is 3.9500e-07, the standard deviation of monomial coefficient is 5.2055e-04, and the standard deviation of constant coefficient is 0.4166.

For uniform pdf block CBE variation curves fitting over 2*2 mm region,in first order polynomial, the mean of slope is 0.0013, and the mean of intercept is 1.9105; the standard standard deviation of slope is 3.5416e-04, and the standard deviation of intercept is 0.7574. In second order polynomial, the mean of quadratic coefficient is -8.5445e-07, the mean of monomial coefficient is 0.0023, and the mean of constant coefficient is 1.6897; the standard deviation of quadratic coefficient is 4.7055e-07, the standard deviation of monomial coefficient is 6.6676e-04, and the standard deviation of constant coefficient is 0.7283. For ratio pdf block CBE variation curves fitting,in first order polynomial, the mean of slope is 9.1229e-04, and the mean of intercept is 1.1809; the standard standard deviation of slope is 3.1397e-04, and the standard deviation of intercept is 0.4984. In second order polynomial, the mean of quadratic coefficient is -5.2366e-07, the mean of monomial coefficient is 0.0016, and the mean of constant coefficient is 1.0457; the standard deviation of quadratic coefficient is 3.9574e-07, the standard deviation of monomial coefficient is 5.1031e-04, and the standard deviation of constant coefficient is 0.4577.

It's obviously that second order polynomial fitting works better than first order polynomial fitting, cause it is closer to the original curve. To verify this, we calculate the error estimates for every region size. Over 6*6 mm, the error estimate of uniform pdf first order polynomial fitting is 0.1274, and it for ratio pdf is 0.0849, the differ is 0.0425. The error estimate of uniform pdf second order polynomial fitting is 0.0822, and it for ratio pdf is 0.0543, the differ is 0.0279. Over 4*4 mm, the error estimate of uniform pdf first order polynomial fitting is 0.1323, and it for ratio pdf is 0.0879, the differ is 0.0444. The error estimate of uniform pdf second order polynomial fitting is 0.0866, and it for ratio pdf is 0.0567, the differ is 0.0299. Over 2*2 mm, the error estimate of uniform pdf first order polynomial fitting is 0.1392, and it for ratio pdf is 0.0921, the differ is 0.0480. The error estimate of uniform pdf second order polynomial fitting is 0.0956, and it for ratio pdf is 0.0631, the differ is 0.0325. In parallel, we can find that with the same data, ratio pdf CBE fitting mean error square is less than uniform pdf CBE fitting mean error square. Over 6*6 mm, mean error square of uniform pdf first order polynomial fitting is 0.0164, and it for ratio pdf is 0.0076, the differ is 0.0088. The mean error square of uniform pdf second order polynomial fitting is 0.0063, and it for ratio pdf is 0.0027, the differ is 0.0036. Over 4*4 mm, mean error square of uniform pdf first order polynomial fitting is 0.0178, and it for ratio pdf is 0.0083, the differ is 0.0095. The mean error square of uniform pdf second order polynomial fitting is 0.0070, and it for ratio pdf is 0.0030, the differ is 0.0040. Over 2*2 mm, mean error square of uniform pdf first order polynomial fitting is 0.0196, and it for ratio pdf is 0.0088, the differ is 0.0108. The mean error square of uniform pdf second order polynomial fitting is 0.0087, and it for ratio pdf is 0.0038, the differ is 0.0049. All these data approves that CBE with ratio pdf is more nearly linear than with uniform pdf. Ratio pdf has a higher degree of fitting, indirectly shows that it has less noises.

VI. Appendix

A. *block.m*

```
% Function name: Piexl & Block & Interpolation
% Descript: generate uniform and rpdf CBE blocks, interpolations and variation curves
% Input: CBE valus from 'td714_cberesult.mat'
% Output: CBE Blocks, CBE Interpolations, CBE Variation Curves
% Author: Jie Li
% Data: 9/21/2015

%% Initialization
clear all; close all
currentpath = pwd;
test_num = currentpath(end-4:end);

% Load data
resultfolder=[pwd '/result'];
cd (resultfolder);
load td714_cberesult.mat;
cbmin=min(min(min(cbestd)));
cbmax=max(max(max(cbestd)));
mtxCbestd=size(cbestd);
cbecols = 1:mtxCbestd(3);
cberows = 1:mtxCbestd(2);

% Set Values
ht=6;wd=6;
sos=1.54; srate=24;
xunit=38/127; yunit=sos./2./srate;

% Block size
[rr,cc]=size(squeeze(cbestd(1,:,:)));
inx=wd/xunit; iny=ht/yunit;
roiy=[1:round(iny):rr,rr]; roix=[1:round(inx):cc,cc];

sunif=zeros((length(roix)-2)*(length(roiy)-2),40);
srpdf=zeros((length(roix)-2)*(length(roiy)-2),40);


%% Main Blocks
for sk=1:40
    number=0;
    for kk=1:length(roix)-2
        for ll=1:length(roiy)-2;
            sumcbe=0;sumcberpdf=0;i=0;
            for  xx=1:round(inx);
                for yy=1:round(iny);
                    cbeblkvalue=cbestd(sk, (ll-1)*round(iny)+(rr-round(iny)*(length(roiy)-2))+yy, ...
                        (kk-1)*round(inx)+round((cc-round(inx)*(length(roix)-2))/2)+xx);
                    cberpdfblkvalue=cbestdrpdf(sk, ...
                        (ll-1)*round(iny)+(rr-round(iny)*(length(roiy)-2))+yy, ...
                        (kk-1)*round(inx)+round((cc-round(inx)*(length(roix)-2))/2)+xx);
                    i=i+1;
                    sumcbe=sumcbe+cbeblkvalue;
                    sumcberpdf=sumcberpdf+cberpdfblkvalue;
                end
            end
            number=number+1;
            cbeblk(sk,ll,kk)=sumcbe/i;
            sunif(number,sk)=sumcbe/i;
            cbeblkrpdf(sk,ll,kk)=sumcberpdf/i;
            srpdf(number,sk)=sumcberpdf/i;
        end
    end
end

save([test_num '_blockresult.mat']);



%% LOAD THE ALREADY SAVED RESULT
load ([test_num '_blockresult.mat']);

cbeblkrows=(rr-round(iny)*(length(roiy)-2))+round(iny/2)+1:rr-round(iny/2);
```

```
cbeblkcols=round((cc-round(inx)*(length(roix)-2))/2)+round(inx/2)+1: ...
    cc-round((cc-round(inx)*(length(roix)-2))/2)-round(inx/2);

cbeblkinterrows=(rr-round(iny)*(length(roiy)-2))+1:rr;
cbeblkintercols=round((cc-round(inx)*(length(roix)-2))/2)+1: ...
    cc-round((cc-round(inx)*(length(roix)-2))/2);

% Plot Piexl, Blocks and  Interpolation
for sk=[1,10,20,40]

    figure;  imagesc(cbecols,cberows,squeeze(cbestd(sk,:,:)));
    colormap(cbeclr);colorbar;caxis([0 6]);
    title(sprintf('%s : Uniform PDF CBE at Frame %i',test_num, sk),'FontWeight','bold','FontSize',20);
    set(gca,'FontSize',20,'FontWeight','bold');

    figure;  imagesc(cbecols,cberows,squeeze(cbestdrpdf(sk,:,:)));
    colormap(cbeclr);colorbar; caxis([-0.4 4.8]);
    title(sprintf('%s : Ratio PDF CBE at Frame %i',test_num, sk),'FontWeight','bold','FontSize',20);
    set(gca,'FontSize',20,'FontWeight','bold');

    figure; imagesc(cbeblkcols,cbeblkrows,squeeze(cbeblk(sk,:,:)));colormap(cbeclr); colorbar; ...
        caxis([0 6]);
    title(sprintf('%s : Uniform PDF CBE Block at Frame %i',test_num, ...
        sk),'FontWeight','bold','FontSize',20);
    set(gca,'FontSize',20,'FontWeight','bold');

    figure; imagesc(cbeblkcols,cbeblkrows,squeeze(cbeblkrpdf(sk,:,:)));
    colormap(cbeclr); colorbar; caxis([-0.4 4.8]);
    title(sprintf('%s : Ratio PDF CBE Block at Frame %i',test_num, ...
        sk),'FontWeight','bold','FontSize',20);
    set(gca,'FontSize',20,'FontWeight','bold');

    cbeblki=interp2(squeeze(cbeblk(sk,:,:)),4,'cubic');
    figure; imagesc(cbeblkintercols,cbeblkinterrows,cbeblki);colormap(cbeclr); colorbar; caxis([0 6]);
    title(sprintf('%s : Uniform PDF CBE Interpolation at Frame %i',test_num, ...
        sk),'FontWeight','bold','FontSize',20);
    set(gca,'FontSize',20,'FontWeight','bold');

    cbeblkrpdfi=interp2(squeeze(cbeblkrpdf(sk,:,:)),4,'cubic');
    figure; imagesc(cbeblkintercols,cbeblkinterrows,cbeblkrpdfi);
    colormap(cbeclr); colorbar; caxis([-0.4 4.8]);
    title(sprintf('%s : Ratio PDF CBE Interpolation at Frame %i',test_num, ...
        sk),'FontWeight','bold','FontSize',20);
    set(gca,'FontSize',20,'FontWeight','bold');
end


%% variance curve
a=30:30:1200;
sumunifcbe=0;
sumratiocbe=0;
figure;
for i=1:1:ll*kk
    plot(a,sunif(i,:),'r');hold on; plot(a,srpdf(i,:),'k');grid on;title(sprintf('td714 : Uniform ...
        and Ratio PDF Block CBE Variation Curve'),'FontWeight','bold','FontSize',16);
    set(gca,'FontSize',16,'FontWeight','bold');xlabel('time (sec)');ylabel('CBE ...
        (dB)');legend('Uniform PDF Block CBE','Ratio PDF Block CBE','Location','northwest');
    hold on;
    sumunifcbe=sumunifcbe+sunif(i,:);
    sumratiocbe=sumratiocbe+srpdf(i,:);
end

meanunifcbe=sumunifcbe/(ll*kk);
meanratiocbe=sumratiocbe/(ll*kk);


% coefficients and estimations
for i=1:1:ll*kk
    [pu1sample,pu1ssample] = polyfit(a,sunif(i,:),1);
    pu1(i,:)=pu1sample;
    [ypu1,Δpu1]=polyval(pu1sample,a,pu1ssample);
    yu1(i,:) = ypu1;
    errorpu1(i,:)=sum(Δpu1)/40;

    [pr1sample,pr1ssample] = polyfit(a,srpdf(i,:),1);
    pr1(i,:)=pr1sample;
    [ypr1,Δpr1]=polyval(pr1sample,a,pr1ssample);
```

```
    yr1(i,:) = ypr1;
    errorpr1(i,:)=sum(Δpr1)/40;

    [pu2sample,pu2ssample] = polyfit(a,sunif(i,:),2);
    pu2(i,:)=pu2sample;
    [ypu2,Δpu2]=polyval(pu2sample,a,pu2ssample);
    yu2(i,:) = ypu2;
    errorpu2(i,:)=sum(Δpu2)/40;

    [pr2sample,pr2ssample] = polyfit(a,srpdf(i,:),2);
    pr2(i,:)=pr2sample;
    [ypr2,Δpr2]=polyval(pr2sample,a,pr2ssample);
    yr2(i,:) = ypr2;
    errorpr2(i,:)=sum(Δpr2)/40;
end

% standard deviation
stdpu11=std (pu1(:,1));
stdpu12=std (pu1(:,2));
stdpu21=std (pu2(:,1));
stdpu22=std (pu2(:,2));
stdpu23=std (pu2(:,3));
stdpr11=std (pr1(:,1));
stdpr12=std (pr1(:,2));
stdpr21=std (pr2(:,1));
stdpr22=std (pr2(:,2));
stdpr23=std (pr2(:,3));

% first order fitting
figure;
for i=1:1:ll*kk
    plot(a,yu1(i,:),'r');hold on; plot(a,yr1(i,:),'k');grid on;title(sprintf('td714 : Uniform and ...
        Ratio PDF Block CBE First Order Variation Curve'),'FontWeight','bold','FontSize',15);
    set(gca,'FontSize',16,'FontWeight','bold');xlabel('time (sec)');ylabel('CBE ...
        (dB)');legend('Uniform PDF Block CBE','Ratio PDF Block CBE','Location','northwest');
    hold on;
end

% first order error bar
figure;
x=1:1:ll*kk;
yu1slope=pu1(:,1);
erroryu1slope=std(yu1slope)*ones(size(x));
errorbar(x,yu1slope,erroryu1slope,'r');
hold on;grid on;
yr1slope=pr1(:,1);
erroryr1slope=std(yr1slope)*ones(size(x));
errorbar(x,yr1slope,erroryr1slope,'k');
title({'td714 : Uniform and Ratio PDF First Order';'Polynomial Slope ...
    Error'},'FontWeight','bold','FontSize',20);
set(gca,'FontSize',20,'FontWeight','bold');
xlabel('Region Number');ylabel('Slope');legend('Uniform pdf','Ratio ...
    pdf','Location','northwest');xlim([0 ll*kk+1]);

figure;
x=1:1:ll*kk;
yu1intercept=pu1(:,2);
erroryu1intercept=std(yu1intercept)*ones(size(x));
errorbar(x,yu1intercept,erroryu1intercept,'r');
hold on;grid on;
yr1intercept=pr1(:,2);
erroryr1intercept=std(yr1intercept)*ones(size(x));
errorbar(x,yr1intercept,erroryr1intercept,'k');
title({'td714 : Uniform and Ratio PDF First Order';'Polynomial Intercept ...
    Error'},'FontWeight','bold','FontSize',20);
set(gca,'FontSize',20,'FontWeight','bold');
xlabel('Region Number');ylabel('Intercept');legend('Uniform pdf','Ratio pdf');xlim([0 ll*kk+1]);


%second order fitting
figure;
for i=1:1:ll*kk
    plot(a,yu2(i,:),'r');hold on; plot(a,yr2(i,:),'k');grid on;title(sprintf('td714 : Uniform and ...
        Ratio PDF Block CBE Second Order Variation Curve'),'FontWeight','bold','FontSize',15);
    set(gca,'FontSize',16,'FontWeight','bold');xlabel('time (sec)');ylabel('CBE ...
        (dB)');legend('Uniform PDF Block CBE','Ratio PDF Block CBE','Location','northwest');
    hold on;
```

```
end

%second order error bar
figure;
x=1:1:ll*kk;
yu2quadratic=pu2(:,1);
erroryu2quadratic=std(yu2quadratic)*ones(size(x));
errorbar(x,yu2quadratic,erroryu2quadratic,'r');
hold on;grid on;
yr2quadratic=pr2(:,1);
erroryr2quadratic=std(yr2quadratic)*ones(size(x));
errorbar(x,yr2quadratic,erroryr2quadratic,'k');
title({'td714 : Uniform and Ratio PDF Sirst Order Polynomial';' Quadratic Coefficient ...
    Error'},'FontWeight','bold','FontSize',18);
set(gca,'FontSize',18,'FontWeight','bold');
xlabel('Region Number');ylabel('Quadratic Coefficient');legend('Uniform pdf','Ratio ...
    pdf','Location','northwest');xlim([0 ll*kk+1]);

figure;
x=1:1:ll*kk;
yu2monomial=pu2(:,2);
erroryu2monomial=std(yu2monomial)*ones(size(x));
errorbar(x,yu2monomial,erroryu2monomial,'r');
hold on;grid on;
yr2monomial=pr2(:,2);
erroryr2monomial=std(yr2monomial)*ones(size(x));
errorbar(x,yr2monomial,erroryr2monomial,'k');
title({'td714 : Uniform and Ratio PDF Second Order Polynomial';'Monomial Coefficient ...
    Error'},'FontWeight','bold','FontSize',18);
set(gca,'FontSize',18,'FontWeight','bold');
xlabel('Region Number');ylabel('Monomial Coefficient');legend('Uniform pdf','Ratio pdf');xlim([0 ...
    ll*kk+1]);

figure;
x=1:1:ll*kk;
yu2constant=pu2(:,3);
erroryu2constant=std(yu2constant)*ones(size(x));
errorbar(x,yu2constant,erroryu2constant,'r');
hold on;grid on;
yr2constant=pr2(:,3);
erroryr2constant=std(yr2constant)*ones(size(x));
errorbar(x,yr2constant,erroryr2constant,'k');
title({'td714 : Uniform and Ratio PDF Second Order Polynomial';' Constant Coefficient ...
    Error'},'FontWeight','bold','FontSize',18);
set(gca,'FontSize',18,'FontWeight','bold');
xlabel('Region Number');ylabel('Constant Coefficient');legend('Uniform pdf','Ratio ...
    pdf','Location','north');xlim([0 ll*kk+1]);



% error_polyval_Δ
blocknumber=1:ll*kk;

figure;plot(blocknumber,errorpu1,'r');hold on;plot(blocknumber,errorpr1,'k');
grid on;title(sprintf('td714 : First Order Polynomial Error ...
    Estimates'),'FontWeight','bold','FontSize',20);
set(gca,'FontSize',20,'FontWeight','bold');xlabel('Region Number');ylabel('Error ...
    Estimates');legend('Uniform PDF','Ratio PDF');xlim([0 ll*kk+1]);

figure;plot(blocknumber,errorpu2,'r');hold on;plot(blocknumber,errorpr2,'k');
grid on;title(sprintf('td714 : Second Order Polynomial Error ...
    Estimates'),'FontWeight','bold','FontSize',20);
set(gca,'FontSize',20,'FontWeight','bold');xlabel('Region Number');ylabel('Error ...
    Estimates');legend('Uniform PDF','Ratio PDF');xlim([0 ll*kk+1]);

meanerrorpu1=sum(errorpu1)/(ll*kk);
meanerrorpr1=sum(errorpr1)/(ll*kk);
meanerrorpu2=sum(errorpu2)/(ll*kk);
meanerrorpr2=sum(errorpr2)/(ll*kk);

% error square
for i=1:1:ll*kk
    pu1errorsquare(i,1)=sum((yu1(i,:) - sunif(i,:)).*(yu1(i,:) - sunif(i,:)));
    pr1errorsquare(i,1)=sum((yr1(i,:) - srpdf(i,:)).*(yr1(i,:) - srpdf(i,:)));
    pu2errorsquare(i,1)=sum((yu2(i,:) - sunif(i,:)).*(yu2(i,:) - sunif(i,:)));
    pr2errorsquare(i,1)=sum((yr2(i,:) - srpdf(i,:)).*(yr2(i,:) - srpdf(i,:)));
end
```

```
276
277
278 % error square mean
279 meanpu1errorsquare=(pu1errorsquare(:,1))/40;
280 meanpr1errorsquare=(pr1errorsquare(:,1))/40;
281 meanpu2errorsquare=(pu2errorsquare(:,1))/40;
282 meanpr2errorsquare=(pr2errorsquare(:,1))/40;
283
284 blocknumber=1:ll*kk;
285 figure;plot(blocknumber,meanpu1errorsquare,'r');hold on;plot(blocknumber,meanpr1errorsquare,'k');
286 grid on;title(sprintf('td714 : First Order Polynomial Square ...
        Error'),'FontWeight','bold','FontSize',20);
287 set(gca,'FontSize',20,'FontWeight','bold');xlabel('Region Number');ylabel('Square ...
        Error');legend('Uniform PDF','Ratio PDF');xlim([0 ll*kk+1]);
288
289 figure;plot(blocknumber,meanpu2errorsquare,'r');hold on;plot(blocknumber,meanpr2errorsquare,'k');
290 grid on;title(sprintf('td714 : Second Order Polynomial Square ...
        Error'),'FontWeight','bold','FontSize',20);
291 set(gca,'FontSize',20,'FontWeight','bold');xlabel('Region Number');ylabel('Square ...
        Error');legend('Uniform PDF','Ratio PDF');xlim([0 ll*kk+1]);
292
293
294 totalmeanpu1errorsquare=sum(meanpu1errorsquare)/(ll*kk);
295 totalmeanpr1errorsquare=sum (meanpr1errorsquare)/(ll*kk);
296 totalmeanpu2errorsquare=sum(meanpu2errorsquare)/(ll*kk);
297 totalmeanpr2errorsquare=sum(meanpr2errorsquare)/(ll*kk);
```

REFERENCES

[1] RJ Stafford and BA Taylor, "Practical clinical thermometry", in *Physics of Thermal Therapy: Fundamentals and Clinical Applications*, EG Moros, Ed., Imaging In Medical Diagnosis And Therapy, chapter 3, pp. 41–44. Taylor & Francis, 2012.

[2] Joonho Seo, Sun Kwon Kim, Young sun Kim, Kiwan Choi, Dong Geon Kong, and Won-Chul Bang, "Motion compensation for ultrasound thermal imaging using motion-mapped reference model: An in vivo mouse study", in *Biomedical Engineering, IEEE Transactions*, vol. 61. IEEE, 2014.

[3] RM Arthur, D Basu, YZ Guo, JW Trobaugh, and EG Moros, "Temperature dependence of ultrasonic backscattered energy in images compensated for tissue motion", in *IEEE TRANSACTIONS ON ULTRASONICS FERROELECTRICS AND FREQUENCY CONTROL*, vol. 57. 2010.

[4] RM Arthur, "Temperature imaging using ultrasound", in *Physics of Thermal Therapy: Fundamentals and Clinical Applications*, EG Moros, Ed., Imaging In Medical Diagnosis And Therapy, chapter 13, pp. 1–15. Taylor & Francis, 2012.

[5] CA Damianou, NT Sanghvi, FJ Fry, and R Maass-Moreno, "Dependence of ultrasonic attenuation and absorption in dog soft tissues on temperature and thermal dose", in *J Acoust Soc Am*, vol. 102, pp. 628–634. 1997.

[6] M Ribault, J Chapelon, D Cathignol, and A Gelet, "Differential attenuation imaging for the characterization of high intensity focused ultrasound lesions", in *Ultrasonic Imaging*, vol. 20, pp. 160–177. 1998.

[7] RM Arthur, JW Trobaugh, WL Straube, and EG Moros, "Temperature dependence of ultrasonic backscattered energy in motion compensated images", in *Ultrasonics, Ferroelectrics, and Frequency Control, IEEE Transactions*, vol. 52. IEEE, 2005.

[8] RM Arthur, JW Trobaugh, WL Straube, EG Moros, and S Sangkatumvong, "Temperature dependence of ultrasonic backscattered energy in images compensated for tissue motion", in *2003 IEEE Ultrasonics Symposium*, DE Yuhas and SC Schneider, Eds., vol. 1, pp. 990–3 vol.1. 2003.

[9] V Auboiroux, L Petrusca, M Viallon, T Goget, CB Becker, and R Salomir, "Ultrasonography-based 2d motion-compensated hifu sonication integrated with reference-free mr temperature monitoring: a feasibility study ex vivo", in *PHYSICS IN MEDICINE AND BIOLOGY*, vol. 57. 2012.

[10] WL Straube and RM Arthur, "Theoretical estimation of the temperature dependence of backscattered ultrasonic power for noninvasive thermometry", *J Ultrasound in Med & Biol*, vol. 20, pp. 915–922, 1994.

[11] WY Zhao, "Real-time temperature imaging using ultrasonic change in backscattered energy", Master's thesis, Washington Univerity in St.Louis, St. Louis, MO, 2014.

[12] Yuzheng Guo, *A Framework for Temperature Imaging using the Change in Backscattered Ultrasonic Signals*, PhD thesis, Department of Electrical and Systems Engineering, Washington University, St. Louis, MO, 2009, pp. 175.

CONTENTS